MORGENSTERN, N. R. and J. S. TCHALENKO 1967. *Géotechnique* 17: 309–328

MICROSCOPIC STRUCTURES IN KAOLIN SUBJECTED TO DIRECT SHEAR

N. R. MORGENSTERN* and J. S. TCHALENKO*

SYNOPSIS

A clay with near perfect particle parallelism was prepared by consolidating a slurried kaolin in a large oedometer. Shear box samples trimmed at various angles to the compression direction revealed no significant difference in drained strength. Samples with original bedding normal and parallel to the shearing direction were interrupted at various displacements and thin sections prepared after impregnation with Carbowax. The sequence of microscopic shear structures shows that in both cases the features at peak strength result from simple shear conditions and that a continuous horizontal structure appears only towards the residual stage. Intermediate structures are interpreted in terms of the kinematic restraint imposed by the configuration of the box. Detailed examination of the development of kink-bands and compression textures lead to the notion of basal plane slip as the basic mechanism in shear induced structures.

Une argile ayant une orientation préférentielle quasi-parfaite a été préparée en consolidant une boue de kaolinite dans un œdomètre de grand diamètre. Des échantillons de cisaillement direct taillés suivant différentes orientations par rapport à la direction de consolidation produirent des résistances au cisaillement comparables. Des échantillons à litage parallèle et perpendiculaire à la direction de cisaillement furent interrompus à plusieurs étages de déplacement, impregnés de Carbowax et découpés en lames minces pétrographiques. La succession des microstructures de cisaillement montre que dans les deux cas leur aspect à l'instant de la résistance maximum résulte de conditions de cisaillement simple, et qu'une structure horizontale continue n'apparaît que vers la résistance résiduelle. Les structures intermédiares sont interprétées en fonction de la restriction cinématique imposée par la configuration de l'appareil à cisaillement. L'observation détaillée du développement de plis en S (kink-bands) et des textures de compression ammène à envisager le glissement suivant le clivage basique comme le mécanisme de base des structures de cisaillement.

INTRODUCTION

It is convenient to consider the microstructure[1] of a soil to have, in general, two components. The first, which may be termed *original fabric*, has its origin in the composition of the sediment and its sedimentary history. An original fabric will be either random (e.g. Rosenquist, 1959; O'Brien, 1963) or will display a planar preferred orientation. Depositional processes and later diagenetic or tectonic processes can give rise to macrostructural features such as fissures and slickensides which may be extremely important in governing the strength of the soil; but such considerations are outside the scope of this study. If the soil has been subject to post-depositional shear strains it may also exhibit the second component of microstructure which will be called *shear-induced fabric*.

Both original and shear-induced fabrics have a significant influence on the deformation and strength properties of clays. Bishop (1966) and Duncan and Seed (1966a) have reviewed the available data showing that the undrained strength of normally consolidated clay is anisotropic. There is as yet little evidence for anisotropy of effective stress or Hvorslev strength parameters in soft soils. Duncan and Seed (1966b) have, however, shown that the pore pressure parameter A_f depends upon the orientation of the original fabric with respect to the stresses at failure. From their tests on undisturbed London clay, Bishop, Webb and Lewin (1965) also

* Department of Civil Engineering, Imperial College of Science and Technology.

[1] Microstructure has been defined by Morgenstern and Tchalenko (1967a) as those structural features which require the resolving power of at least an optical microscope for their study.

found that the variation of the pore pressures at failure with specimen orientation was a dominant factor in accounting for the anisotropy of the undrained strength of the overconsolidated clay. In the case of rocks (e.g. Chenevert and Gatlin, 1965) both the anisotropy of the cohesion intercept and the angle of shearing resistance have been correlated with the orientation of the original fabric.

Shear straining is also known to induce preferred orientation in clays. Examples of shear-induced fabrics have been given by Williamson (1947), Astbury (1960), Goldstein, Misumsky and Lapidus (1961), Turovskaya (1964) and others. Skempton (1964) drew attention to the decrease in shearing resistance of some clays caused by the development of a continuous band of strongly orientated particles and attributed the residual shear strength of such clays to the presence of this shear-induced structure. Skempton also noted that the shear-induced fabric contained secondary slip domains and an orientated matrix. Morgenstern and Tchalenko (1967c) studied several examples of shear-induced fabrics from the shear zone of landslides and observed that the structures varied with the composition of the soil and the extent of the movement. It is apparent from these and other such observations that the concept of the presence at failure of a single thin zone of orientated clay particles is an unwarranted oversimplification (e.g. Yong and Warkentin, 1966) and that the development of a shear-induced fabric is a process of considerable complication.

It is possible to outline some general principles relating the microstructure and shear deformation behaviour of clays of low sensitivity. Restricting consideration to controlled strain loading of a saturated clay, all clays, regardless of whether they have a random original fabric or not, will respond to loading by stable yielding during which an increment of strain requires a positive stress increment. Stable yielding persists until failure occurs at the maximum principal stress difference. If the original fabric is anisotropic, the pore pressures or volume changes at failure will also, in general, depend upon the orientation of the original fabric with respect to the principal stresses. At or near failure, slip planes will become evident, marking the initiation of the shear-induced fabric. Existing evidence (Gibson, 1951) suggests that the appearance of these planes is controlled by the mobilization of the Hvorslev angle of shearing resistance. Therefore it seems that the exact appearance of the planes with respect to the stress–strain curve depends upon the relative magnitudes and mobilization with respect to strain of the Hvorslev components of strength. After failure, if stable yielding persists, the stress–strain curve is flat. However, for dilatant soils and for soils with clay contents greater than about 30%, unstable yielding occurs requiring a negative stress increment for a positive strain increment. In either case, further shear-induced structures are established

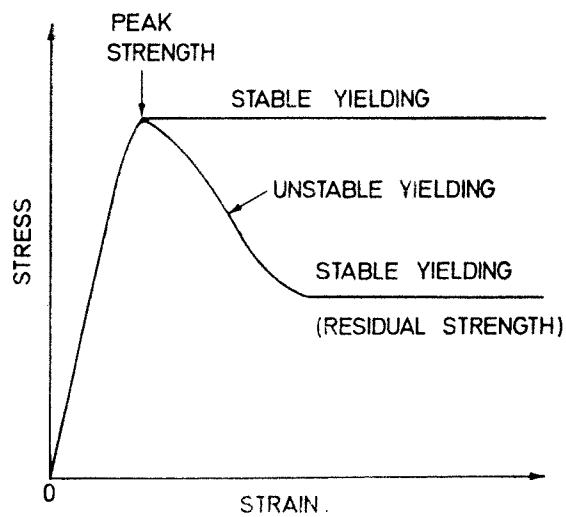

Fig. 1. Stable and unstable yielding

and their pattern will be to a large extent controlled by the restraints on the deformation. Ultimately stable yielding will be re-established at the residual strength where a dominant displacement discontinuity forms which is able to accommodate all further imposed deformation. These features are illustrated in Fig. 1.

The object of this Paper is to study the influence of a known original fabric on the strength of a kaolin and to follow in detail the features of the shear-induced fabric as the kaolin is deformed to its residual shearing resistance. This has been achieved by preparing a series of identical specimens, observing the original fabric, and subjecting them to direct shear under drained conditions in the shear box. Thin sections cut from each of the specimens which have been taken to different strains permit the direct observations of the shear-induced fabric. Details of the testing programme are given in a later section.

It is well known that there are some disadvantages in the use of the shear box for the study of the strength of soils. As Hvorslev (1960) pointed out, failure is progressive and the stress conditions are not known to a high degree of accuracy. Moreover, even in an idealized shear box, there is still debate as to how the results should be interpreted. However, at least at the residual strength, both the shear box and triaxial compression apparatus yield essentially the same results (Petley, 1966) and in this investigation there are some advantages other than its simplicity in the use of the shear box. It is possible to take the specimens to larger strains than can commonly be obtained with triaxial equipment. All the structural information is contained in a central vertical plane parallel to the shear force. Also, since the orientation of the shear-induced structures is being observed directly, evidence may be provided in favour of one or the other interpretations of the shear box.

An essential feature of the shear box test is the presence of restraint. As will be seen, the inclination of shear planes at failure in the shear box is not in the direction of the imposed relative displacement. Slip along these planes is therefore impeded in contrast to the conditions of the triaxial test. Since kinematic restraints also exist in most engineering situations it is of considerable interest to study the post-failure behaviour of a clay subject to such restraints.

TERMINOLOGY

A shear-induced fabric is in general composed of domains, in which the fabric is homogeneous, separated by discontinuities. The size attributed to a domain may vary with the resolving power of the method used in the study of the fabric. In order to describe a shear-induced fabric and discuss its change under further loading, three types of terminology are necessary. These may be called kinematic, sequential and mechanistic. Such considerations have been the subject of considerable attention by structural geologists and the work of Sander (1948), Paterson and Weiss (1961) and Turner and Weiss (1963) is particularly useful in assisting in the formulation of terminology suitable for the study of microstructure in clays.

The kinematic terminology is necessary to describe the structural features which are present in the fabric and which provide the means whereby the material deforms. Following Turner and Weiss (1963) it is convenient to distinguish between two limiting kinds of kinematic discontinuities: *displacement discontinuities* and *strain discontinuities*. For elastic deformation of a homogeneous clay mass neither of these discontinuities will exist. The strain at any point now is in principle deducible from the equilibrium of the mass, the boundary conditions and the appropriate constitutive equation. However, irreversible deformation even in the range of stable yielding, is associated with relative slip between particles. At lower levels of magnification this slip may manifest itself either as a strain or displacement discontinuity when the deformation is non-homogeneous. Examples of strain and displacement discontinuities are shown in Fig. 2. It is important to note that a feature called a displacement or strain discontinuity at a particular level of investigation may itself be reducible to a system of strain

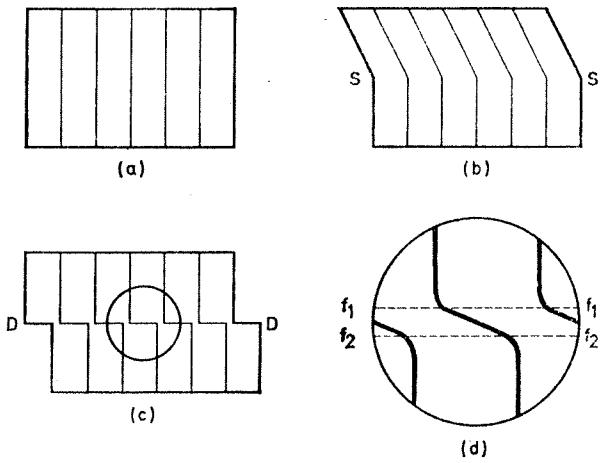

Fig. 2. Types of discontinuity in deformation
(a) unstrained state
(b) strain discontinuity SS
(c) displacement discontinuity DD
(d) magnification of central portion of DD showing two strain discontinuities f_1f_1 and f_2f_2

or displacement discontinuities at a higher level of magnification. An example of this is given in Figs 2(c) and (d).

The sequential terminology describes the order of appearance in time of the kinematic discontinuities and other features of the fabric. This may be achieved by adopting a notation $S_1, S_2 \ldots S_n$, where S_1 is the first feature to be observed, S_2 is the second, and S_n is the last.[2] Where a structure such as S_3 appears to be reducible to a set of sub-structures, the notation S_{3a}, S_{3b} will be used. Original fabric features such as bedding will invariably be S_1.

The mechanistic terminology relates a particular kinematic discontinuity with the orientation and magnitude of the stresses which act upon it. For example, when a cylinder of clay is compressed in the laboratory a conjugate pattern of shear planes is commonly observed as predicted by the Mohr–Coulomb failure criterion and it is known (Gibson, 1951) that the inclination of these planes is best accounted for in terms of the Hvorslev angle of shearing resistance. Skempton (1966) introduced a mixed terminology which incorporated several mechanistic terms that will be adopted here. This mixed terminology has been used by Skempton to describe some tectonic shear zones and by Morgenstern and Tchalenko (1967c) to describe some shear zones from landslides. The mechanistic terms are *Riedel shears*, *thrust shears*, and *tension fractures*. The definition of a *principal displacement shear* given by Skempton (1966) may also be taken as a mechanistic term if it is restricted to imply that the residual strength is being mobilized along its length as will commonly be the case. Hence the slip surface of a landslide which has moved some distance is a displacement discontinuity and a principal displacement shear. The mechanistic terms suggested so far may well be inadequate to account for the complete process of shearing from the initial failure to the development of a principal displacement shear. However, the adoption of further terms must await detailed descriptions of features which cannot be accounted for by the preceding mechanistic terms.

EXPERIMENTAL PROGRAMME

To simplify the optical studies a monomineralic clay was desirable and kaolin was chosen because its large surface area to thickness ratio suggests a disposition towards orientation under applied load.[3] The optical properties of the kaolin crystal are also known to an acceptable degree of accuracy.

---

[2] This notation is not to be confused with Sander's *S*-surface notation which is restricted to the consideration of only fully penetrative planar structures (Turner and Weiss, 1963).

[3] The kaolin was obtained from English Clays Lovering Pochin and Co. Ltd, St. Austell, Cornwall. Its classification properties are: liquid limit 60%, plastic limit 24%, clay fraction ($<2\,\mu$) 95%, organic content 3–4%.

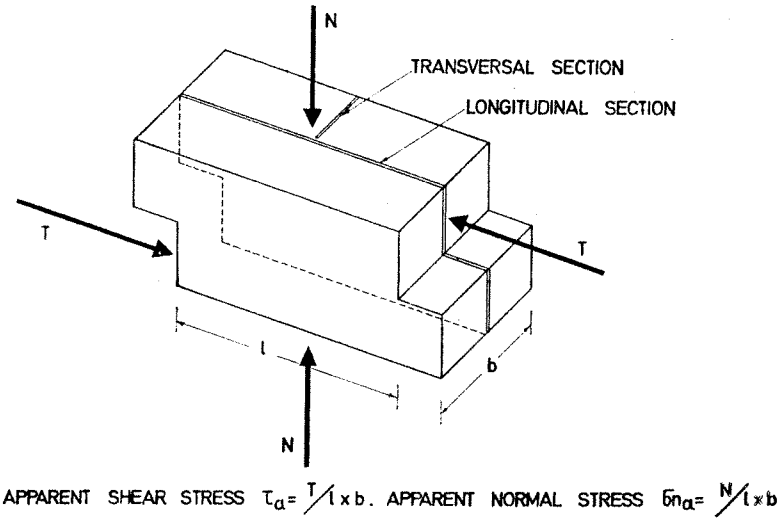

Fig. 3. Planes of thin section and definition of apparent stresses

Dry kaolin was mixed with distilled water to form a slurry with a water content of 100%. After allowing the slurry to age for two weeks, it was poured into a nine inch diameter oedometer and consolidated in conventional increments to an effective pressure of 62·4 lb/sq. in. After unloading the oedometer two sets of shear box specimens were cut from the clay block. Specimen dimensions were 6 cm × 6 cm × 2·5 cm. One set was cut parallel and the other perpendicular to the bedding and each set contained seven specimens. Three inch diameter oedometer specimens were also obtained to provide information regarding the influence of further consolidation on the induced preferred orientation. Detailed structural observations were made on samples deformed in the shear box under a normal load of 31·2 lb/sq. in. Shear

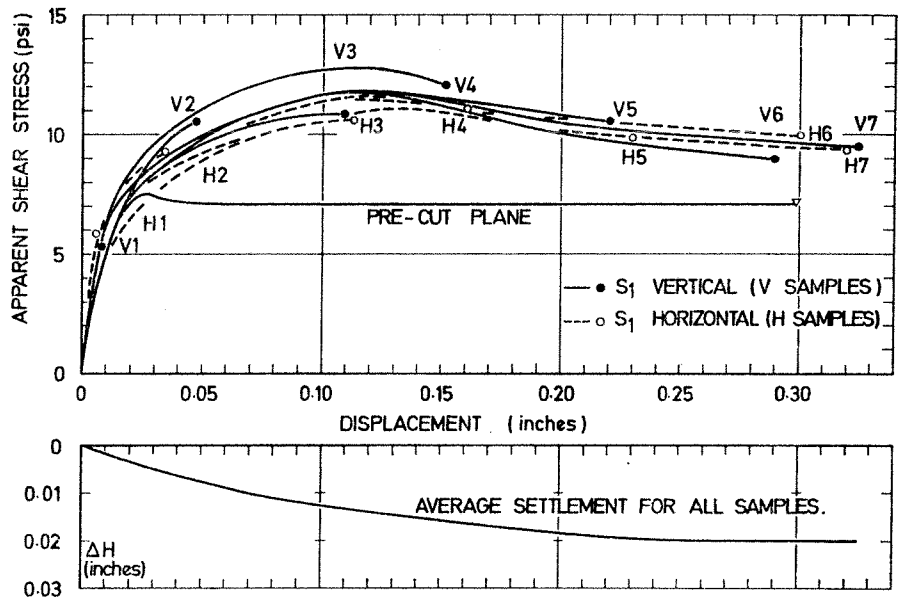

Fig. 4. Shear stress— displacement and settlement curves for drained tests on over-consolidated kaolin. Pre-consolidation load (oedometer) 62·4 lb/sq. in.; normal load in shear box test 31·2 lb/sq. in.

tests were also performed on samples with bedding fixed at different inclinations and on a specimen with a pre-cut plane.

All seven samples of a set were sheared simultaneously at a rate of relative displacement of 0·000115 in./min., which ensured fully drained conditions. Each test was interrupted at a different stage along the apparent shear stress–displacement curve and longitudinal and transversal thin sections were prepared using Carbowax 6000 as an impregnating medium in the manner described by Mitchell (1956). Apparent shear and normal stresses are defined in Fig. 3 which also indicates the planes of the thin sections. In this figure N and T denote the normal and shear forces respectively. Most of the structural information is obtained from the longitudinal sections. The composite apparent shear stress–displacement curves for the tests are shown in Fig. 4 and the positions at which specific tests were terminated are indicated. The residual strength from the specimen containing a pre-cut plane is also shown. It may be noted that the orientation of the original fabric (S_1) has little significant effect on the shearing resistance.

METHOD FOR OPTICAL OBSERVATIONS

A single kaolin crystal is birefringent, and when viewed under crossed nicols in a polarizing microscope with its basal plane parallel to the viewing direction, it behaves like a uniaxial negative crystal. That is, as the crystal is rotated with respect to the direction of the vibration of the wave front emerging from the polarizer it may be seen to transmit zero light intensity when one of the optical axes is parallel to this direction and a maximum light intensity when an optical axis is at 45° to it. Since the optical axes are orthogonal and coincide for all practical purposes with the crystallographic axes, this means that when the trace of the basal plane of the crystal is parallel or orthogonal to the polarizing direction, the crystal is in an extinction position, and when it is at 45° to this direction maximum illumination is observed. As a single crystal is rotated through 360° there are four extinction positions and four positions of maximum illumination. It is also known that a single kaolin crystal displays positive elongation and hence any ambiguity regarding the inclination of the trace of the basal plane may be resolved by viewing with a suitable retardation plate.

Morgenstern and Tchalenko (1967a) have shown that the birefringence of an aggregate of clay particles depends solely upon the intrinsic birefringence of the constituent particles and their spatial configuration. Neither form birefringence nor the presence of Carbowax has any significant effect on the optical response of the aggregate, at least for the porosities of interest in this study.[4] When a random structure is viewed in thin section under crossed nicols, no variation in transmitted light intensity is observed as the section is rotated. If the aggregate has a preferred orientation, the minimum and maximum light intensities will depend upon the degree of orientation. These intensities may be measured and interpreted to give a quantitative measure of the preferred orientation of the aggregate as described by Morgenstern and Tchalenko (1967a). The same equipment and techniques are used for the observations and interpretations reported here.

Details of the shear-induced fabric may be conveniently observed and photographed through the microscope. However, even for the lowest magnification available ($\times 3$) it is not possible to observe the complete section and some discontinuities may be too large for study in this way. In these cases photographs were taken of the complete thin section placed between two sheets of Polaroid. An arrangement, similar in principle, has been adopted by Lafeber and Kurbanovic (1965).

[4] Kaolin impregnated with Carbowax does, however, show an internal linear shrinkage of 0·5 to 1% (Tchalenko, 1967). This manifests itself in cracks which lie parallel to the average particle orientation. These cracks are the dark sub-vertical parallel lines of Figs 5 and 7, and at higher magnifications (e.g. Figs 8 and 15) it may be noted that they do not affect either strain or displacement discontinuities.

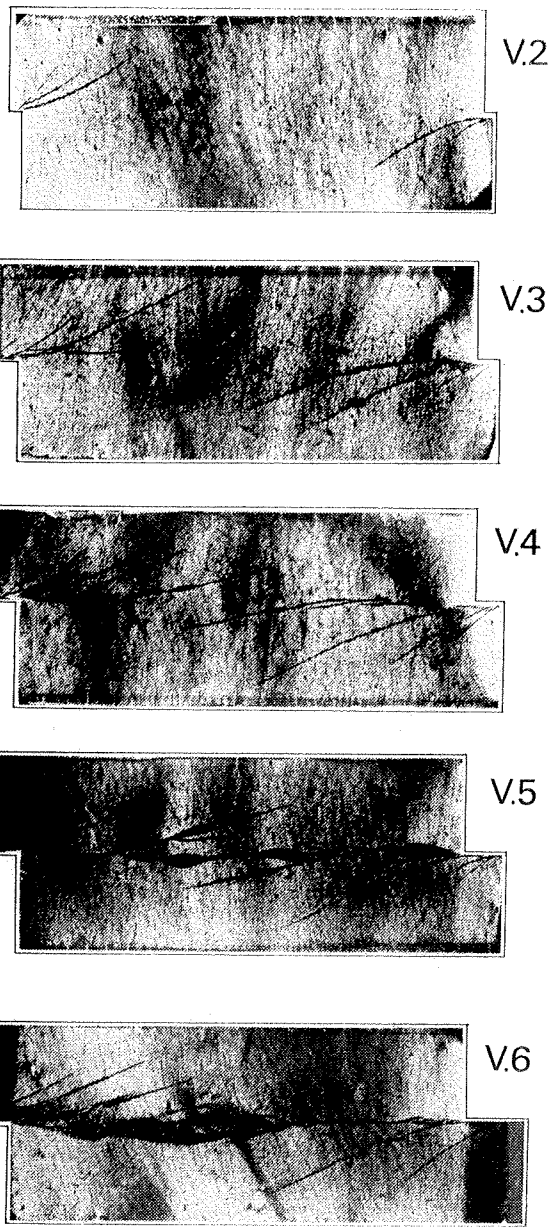

Fig. 5. Sequence of structures in specimens sheared normal to original fabric. Entire longitudinal sections $1 \times 2{\cdot}35$ in. Crossed polars

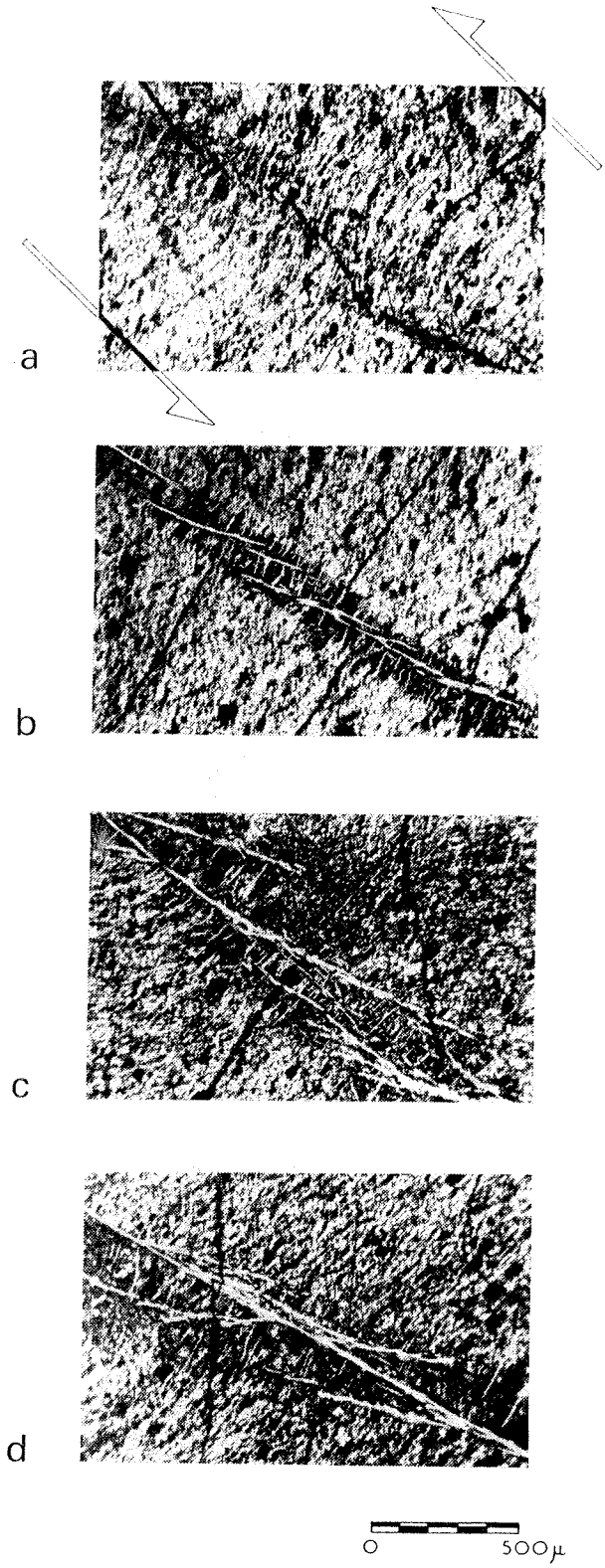

Fig. 7 (left). S_2 discontinuities in specimen V4. Full height (one inch) shown. Crossed polars

Fig. 8 (above). Sequential development of S_2 in specimen with vertical S_1. Horizontal of photographs is $+45°$ in shear box. Half arrows indicate direction of shear. Objective $\times 3$. Crossed polars

Fig. 10 (left). Domain structure resulting from intersection of S_{2a} and S_{2b}, sample V4. Objective × 10. Crossed polars

Fig. 11 (right). S_3 discontinuity in specimen V5. Full height (one inch) shown. Crossed polars

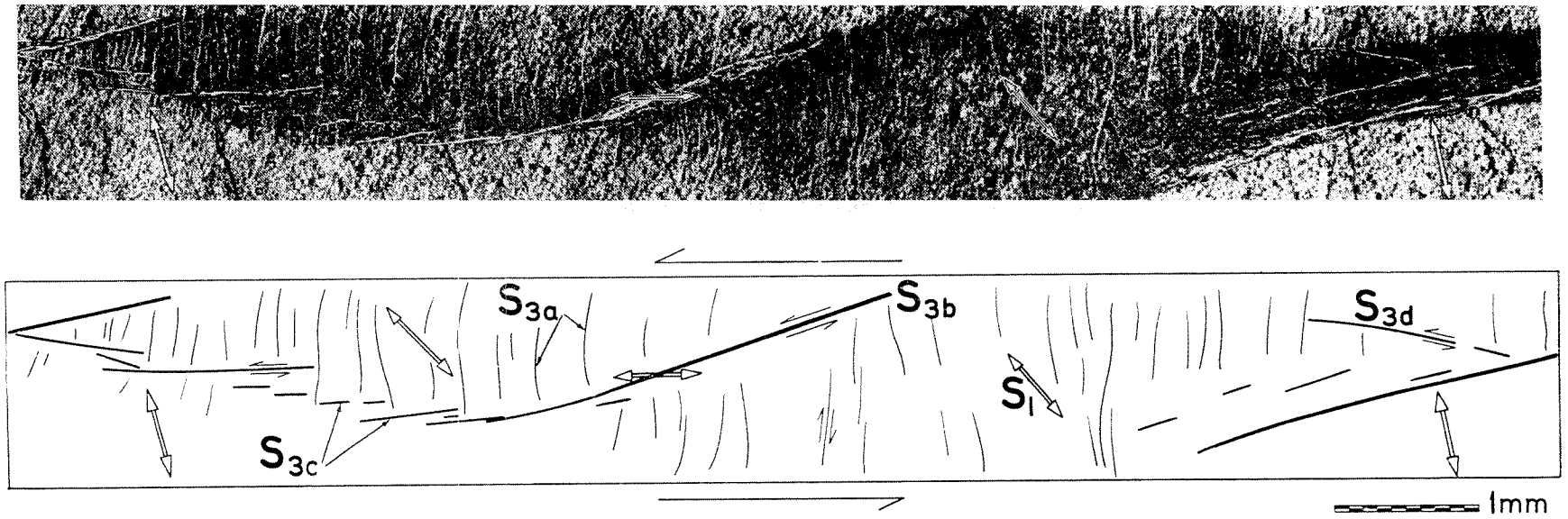

Fig. 12. Detail in S_3 from Fig. 11. Composite of microphotographs. Objective × 3. Crossed polars

SPECIMENS SHEARED NORMAL TO ORIGINAL FABRIC

The original fabric, S_1 was induced by consolidation to 62·4 lb/sq. in. The specimens discussed here were deformed in the shear box under a normal load of 31·2 lb/sq. in. and were aligned so that S_1 was perpendicular to the shear load.

Figure 5 shows a succession of sections taken from specimens interrupted at different stages of the test. The symbol associated with each section in Fig. 5 denotes in Fig. 4 the position on the stress–displacement curve where the test was terminated. The earliest observed manifestation of shear is a rotation of the average particle orientation with respect to the original S_1 direction in the sense of the relative displacement of the two halves of the box.[5] This rotation is not homogeneous over the whole section and is most intense near the edges of the box. Together with this non-homogeneity discontinuities originate at the edges and extend towards the centre. As the displacement increases the discontinuities multiply in a discrete sequence and at diminishing positive angles to the horizontal. Ultimately a continuous zone separating the top from the bottom of the box is created. This general development is illustrated in Fig. 5 and the process will be discussed in more detail. It may be noted here that the loading sides of the box cause high stress concentrations (Kisiel, 1964)

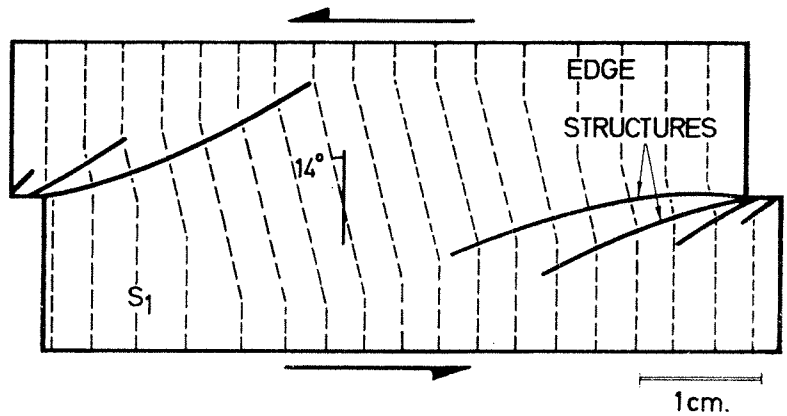

Fig. 6. S_1 rotation prior to peak strength. Specimen V3 (after photograph)

and local straining will therefore be intense. Differential consolidation due to the stress distribution will also cause a non-homogeneous distribution of strength. These effects produce their own structures which will be treated separately. The dominant structures are located over the central two-thirds of the box, where they are reproducible under identical testing conditions and can be followed from section to section. A specimen which had pre-cut planes inclined at 30° to the horizontal at its sides has also been sheared. A thin section revealed that while the local side structures were suppressed the shearing resistance remained unaltered and the dominant structures were essentially reproduced.

In the mid-portion of the specimen prior to peak strength, the fabric undergoes a quasi-homogeneous shear strain as illustrated diagrammatically in Fig. 6. This is facilitated by the edge structures and typically S_1 is rotated by about 14° prior to the formation of the first relevant kinematic discontinuity. Frictional restraint at the top and bottom of the specimen restricts rotation of S_1 as indicated in this figure. At, or immediately after, peak strength, the specimen is penetrated by two kinematic discontinuities which are inclined at about 12° to the horizontal, shown in Fig. 7. These discontinuities are denoted by S_2.

[5] This sense is counter-clockwise in all plates and figures describing shear-induced structures. Measurements of angles are positive in this sense.

The development of S_2 may be followed in detail. The first indication of its formation is a local distortion of S_1. At times this is seen to be accompanied by faint penetrative discontinuities inclined at about 80°–90° to the horizontal. They are seldom more than a few microns wide and have a spacing of 10–50 μ.[6] These structures are S_{2a} and are shown in Fig. 8(a). It may be seen that the S_2 zone is bounded at either side by strain discontinuities which are made prominent by the differential rotation of both S_1 and S_{2a} across the zone. This zone is typically 200–300 μ wide. As motion proceeds further kinematic discontinuities appear *within* S_2 as shown in Fig. 8(b). The onset of their development is already apparent in Fig. 8(a). They consist of a family of displacement discontinuities lying at 12°–14° to S_2 and are denoted by S_{2b}. These discontinuities are observed to form when the rotation of S_1 within the S_2 zone is approximately 30° from its original position. At this stage of the development of S_2, S_{2a} is very apparent and is seen to lie at 95° to S_2. Some of the S_{2a} family have thickened to about double their original width. S_{2b} is about 10 μ wide.[7] It is of interest to observe that the orientation of the particles in these sub-structures is invariably inclined at 0 to −10° to the sub-structures. This has also been observed by Weymouth and Williamson (1953) in their reproduction of the Cloos–Riedel experiment. The sub-structure of S_2 at this

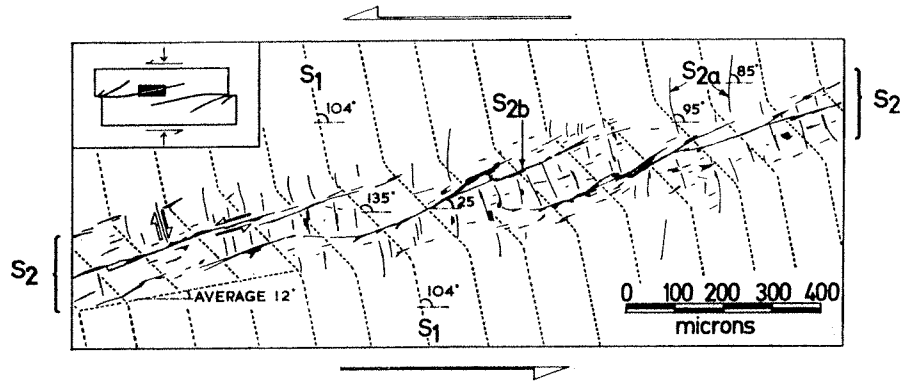

Fig. 9. Detail of discontinuity S_2 in specimen V4

stage is illustrated in Fig. 9. As shown in Fig. 10, S_{2a} and S_{2b} partition the material into rectangular domains.

Subsequent motion produces small displacement discontinuities S_{2c} which interconnect S_{2b} (Fig. 8(c)) and ultimately result in the formation of the continuous displacement discontinuity S_{2d} aligned in the S_2 direction (Fig. 8(d)). It is observed again that the average attitude of the particles is at a few degrees to the structure.

Returning to the gross fabric, it is clear that motion along S_2 is impeded by the restraints due to the testing configuration and this is reflected by the lesser development of S_2 towards the mid-portion of the specimen when compared with that towards the edges. For further displacement to be accommodated the rotation of S_1 between the existing S_2 structures must be increased and new structures must be induced. Fig. 11 gives the shear-induced fabric beyond the peak strength after a displacement of 0·22 in. The dominant new feature to appear is the zone, S_3, connecting the pre-existing S_2 structures. S_3 is bounded by strain discontinuities inclined at about −15° to the horizontal and displacement discontinuities

[6] They possibly originate as slip on discrete planes along S_1 which rotate less than S_1 in the S_2 zone.

[7] If the single kaolin particle is taken to be 0·5 μ in diameter and 0·05 μ thick, then assuming perfect orientation and allowing for void space, many sub-structures such as S_{2b} have room for a stacking of about 100 particles. It is conceivable that this constitutes an average irreducible size of domain with no further shear structures.

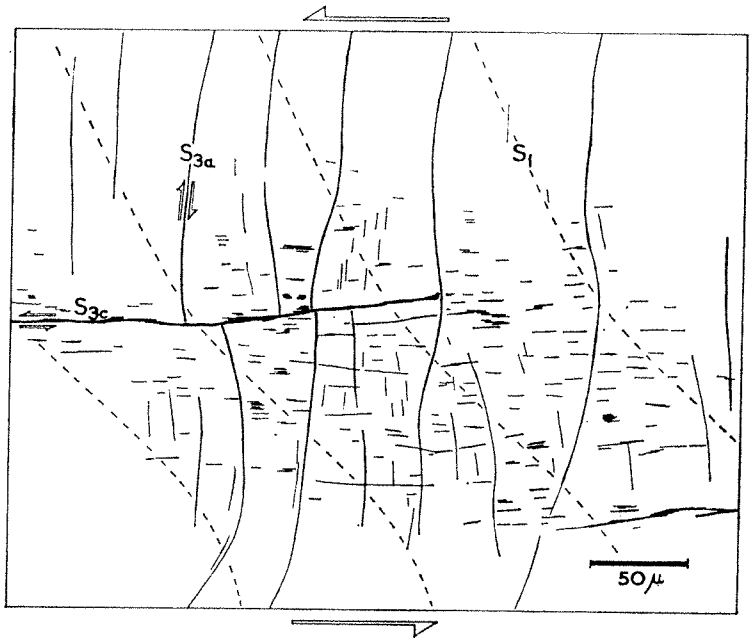

Fig. 13. Non-homogeneous straining around a discontinuity. Specimen V5. A horizontal S_{3c} discontinuity, propagating from left to right, displaces the previously formed sub-vertical S_{3a} structures. The distortion of S_{3a} dies out to the right of S_{3c} (after photograph)

inclined by up to 12° to the horizontal. The combination of the two types of discontinuities produces a sub-horizontal feature of variable thickness.

The sub-structure of S_3 evolves in the following manner. It is noted that S_1 rotates through approximately 45° (Fig. 12). Associated with this rotation is the appearance of the penetrative discontinuities S_{3a} which lie at 85° to the horizontal. An increased local rotation of S_1 and S_{3a} results in the development of displacement discontinuities S_{3b} which are parallel to S_2 and have a spacing of about 2 mm. As shown in Fig. 12, the particle orientation along S_{3b} is essentially horizontal. The imposed displacement can be taken up by slip along S_{3b} and further distortion of S_1 and S_{3a}. If S_{3a} is adopted as a marker structure one may observe that it is discontinuous across the central portion of S_{3c} while severely distorted only at its edges. This is shown in detail in Fig. 13 and suggests that when an active discontinuity is present within the specimen, without extending across its boundaries, its action is like that of a dislocation and straining around it cannot be homogeneous. The next stage in the development of S_3 is the formation of a family of *en echelon* sub-horizontal displacement discontinuities (S_{3c}) which are also evident in Fig. 12. Displacement discontinuities having the attitude of thrust structures (S_{3d}) also appear. The coalescence of all these structures results in S_3.

The similarities in the internal development of S_2 and S_3 are apparent. From a kinematic and a mechanistic point of view S_{2a} is the equivalent of S_{3a}, and S_{2b} is the equivalent of S_{3b}. While S_2 is truly microscopic, S_3 embodies features of both this and almost macroscopic size. The interpretation of the bounding strain discontinuities at $-15°$ presents a special problem which will be discussed later.

The residual strength is approached towards the end of the travel of the shear box. Fig. 14 shows a magnification of the shear zone of specimen V6 at this stage. A displacement discontinuity, S_4 is now present across the specimen. It is a distinctly wavy surface formed by the active parts of S_3 and the portions of S_2 that are flat due to edge effects. Fig. 15 shows the relation between S_{3a} and S_{3b} at the end of travel of the specimen. S_{3a} has been

truncated by the slip along S_{3b} while the increased distortion of the material between these structures has invoked a successive development of S_{3a} discontinuities which all coalesce towards the active displacement discontinuity. Within each S_{3a} fan, near horizontal complementary discontinuities produce rectangular domains with side lengths of 40–100 μ.

SPECIMENS SHEARED PARALLEL TO ORIGINAL FABRIC

These specimens were obtained from the same block of clay as those described previously. They were also sheared under a normal load of 31·2 lb/sq. in. and hence were over-consolidated. The volume changes during shear were identical in both sets of tests but this may be fortuitous.

At peak shear stress both edge structures and S_2 are evident as in the previous sequence. S_2 is found at 20°–25° to the horizontal and has a width of 10 μ. Sub-structures cannot in general be recognized within it. However, strong particle orientation is evident at −10° to −15° to the structure. Up to this stage of relative displacement no rotation of S_1 can be detected. Many shear-induced structures in specimens deformed parallel to S_1 are more difficult to observe because they are thinner by about an order of magnitude. An explanation of this will be given later.

After a displacement of 0·24 in. the zonal structure, S_3, is observed as shown in Fig. 16. It is about 3–4 mm wide and is bounded by thin displacement discontinuities inclined at 11° to the horizontal which are denoted by S_{3b}. Between these displacement discontinuities a penetrative family of kinematic discontinuities inclined at about 85° to the horizontal is clearly evident. This family is composed of a series of strain discontinuities, S_{3a}, which separate zones of different particle orientation. A detail of this remarkable structure is given in Fig. 17. The light and dark bands which give rise to S_{3a} are typically 280 μ and 120 μ wide respectively. The light bands are composed of S_1 which has rotated by about 11°–14° to the horizontal. This is the same as the inclination of S_1 immediately outside S_3. Within the dark bands associated with S_{3a}, the average particle orientation is −40°.[8] The conjunction of the particle orientations in the light and dark bands has the appearance of a kink-band (Dewey, 1965). Within the dark band a sub-structure may be discerned as shown diagramatically in Fig. 18. Its dominant feature is a penetrative family of discontinuities which are of the displacement type (S_{3c}) at about −20° to the horizontal and which sub-divides the zone into bands of about 15 μ width. The particle orientation along these discontinuities is also at −20° to the horizontal. Moreover, S_{3c} can be followed across S_{3a} and is then seen to follow the attitude of S_1. Fig. 18 also shows discontinuities (S_{3d}) at about −12° to S_{3a} which are in the process of formation. The S_{3a} discontinuities terminate distinctly on S_{3b} but beyond S_{3b}, some S_{3c} structures at −20° are found dispersed throughout the material. It is of interest to note that the darker zones away from S_3 shown in Fig. 16 indicate that S_1 is still predominantly horizontal at some distance from the shear zone.

At the end of travel of the shear box, a wavy continuous plane (S_4) has almost developed across the specimen. This is achieved by the mobilization of a few displacement discontinuities which lie between the horizontal and at a low negative angle to it. These structures which originate from the propagation of S_{3c} join the pre-existing S_{3b} discontinuities to form S_4. S_{3a} suffers no apparent further rotation during this process but is cut instead by the slip along S_4. Fig. 19 clearly demonstrates that S_4 acts as a displacement discontinuity when it is fully formed. The imposed displacement is now being accommodated in a width of about 10 μ and the average particle orientation within S_4 is about −15° to −20° to it.

[8] Maximum optical contrast between two adjacent zones each having a different average particle orientation may be achieved when the difference between the two directions of preferred orientation is 45°. The angle here is about 52°.

Fig. 14 (top left). S_4 discontinuity in specimen V6. Full height (one inch) shown. Crossed polars

Fig. 15 (middle left). S_{3a} structures truncated by S_{3b}. Specimen V6. Objective $\times 3$. Crossed polars

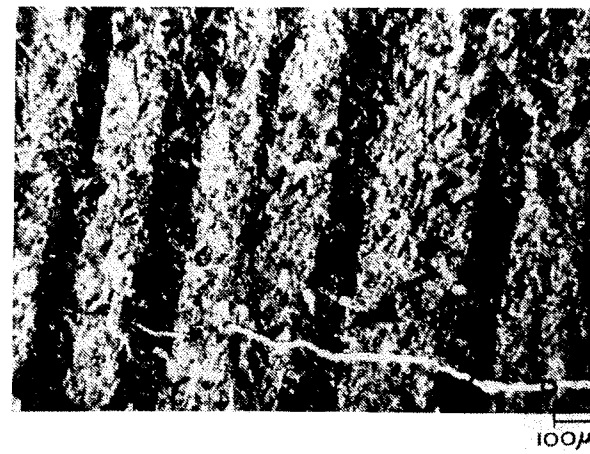

Fig. 16 (bottom left). S_3 zone in specimen H5. Full height (one inch) shown. Crossed polars

Fig. 17 (above). S_{3a} discontinuities in specimen H5. Detail from Fig. 16. Objective $\times 3$. Crossed polars

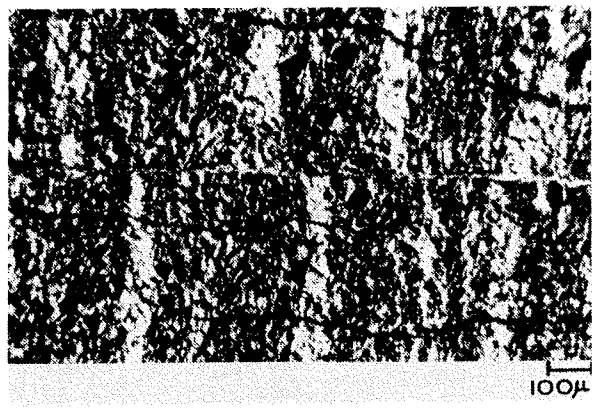

Fig. 19. S_{3a} structures truncated by S_{3c}. Specimen H6. Objective × 3. Crossed polars

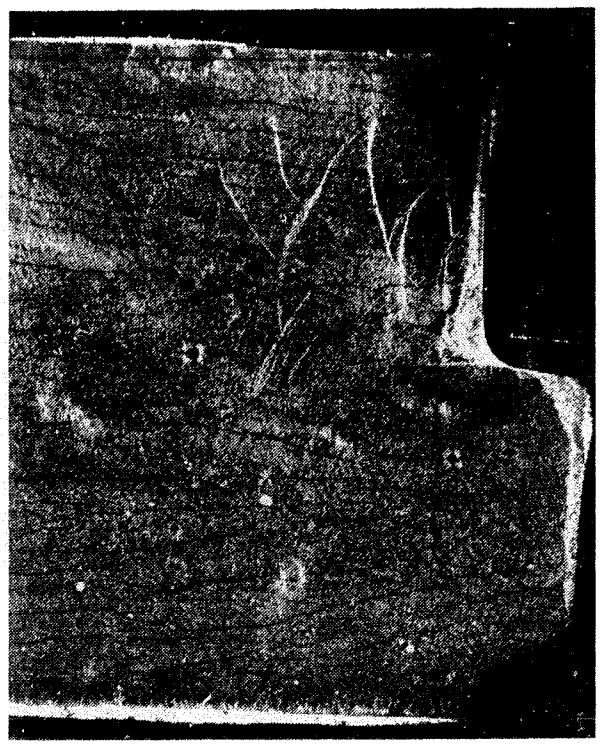

Fig. 20. Edge structures in specimen H4. Full height (one inch) shown. Crossed polars

Fig. 26. Shear zone in pre-cut plane specimen. S_1 originally vertical. Horizontal of photograph is +45° in shear box. Objective × 10. Crossed polars

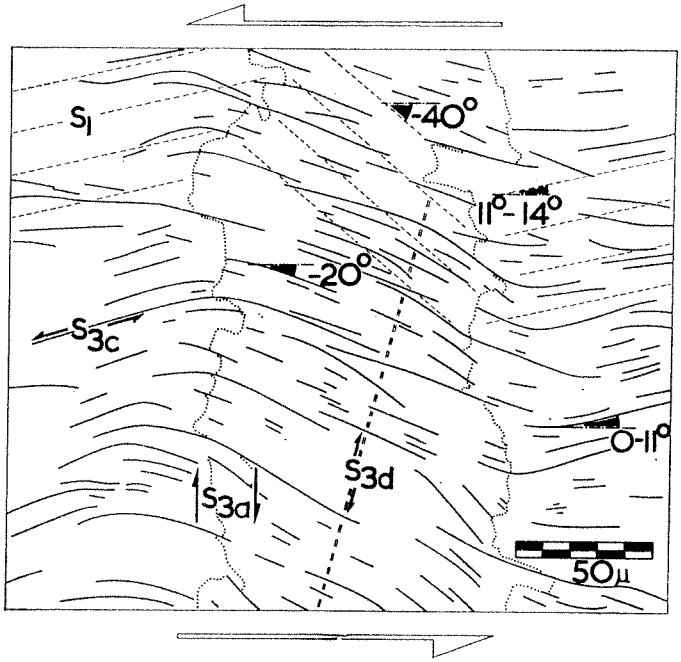

Fig. 18. Detail of kink-band structure S_3. Sample H5

EDGE STRUCTURES

So far, the description of the shear-induced fabric has been concerned primarily with the central portion of the specimen which controls the peak and post-peak shearing resistance of the material. The high stress concentrations and kinematic restraint at the edges of the specimen produce certain structures and some of these may be noted here. In Fig. 5, discontinuities may be seen at high angles to the horizontal. The steepest of these appears at an early stage of the test, and as displacement proceeds its development is arrested as a new one forms at a lower angle. This succession continues to peak strength when S_2 is formed. The sub-structure in all of these edge structures is similar to that of S_2.

The vertical loading edges of the shear box transmit a high compression into the adjacent material. For specimens with a horizontal S_1, a pattern of curvilinear discontinuities forms to produce a slip-line field. An example is given in Fig. 20. This pattern has not been found in specimens with vertical S_1 which may tend locally to consolidate more in the direction of lateral loading.

INTERPRETATION OF OBSERVATIONS

The description of shear-induced fabrics refers to kaolin sheared under a normal load of 31·2 lb/sq. in. after being consolidated in an oedometer to 62·4 lb/sq. in. from an initial water content of 100%. The shear stress–displacement curve to the end of travel of the shear box is essentially independent of the orientation of the apparent shear stress with respect to S_1. This is true not only for the two series of tests when S_1 was horizontal and vertical, but also of tests carried out at the same normal stress with S_1 at 15° and 105° to the horizontal. Two sets of shear tests with vertical and horizontal S_1 carried out at a normal stress of 62·4 lb/sq. in. also failed to reveal any marked anisotropy in the resistance of the clay. Moreover, the shear-induced fabrics of all the tests mentioned have certain features in common, and these are of particular interest since they are likely to be fundamental to the process of distortion of a clay, at least after peak strength.

Original fabric

The degree of orientation of S_1 before shearing must be studied since, if this is intense, it might reasonably be expected to create an anisotropy of resistance in terms of effective stress. Morgenstern and Tchalenko (1967a, b) have shown how the ratio of the transmitted intensities of a thin section in its extinction and illumination positions may be used to assess the degree of orientation in terms of the orientation ratio (R). After consolidating to 62·4 lb/sq. in. from an initial water content of 100% the orientation ratio is 0·02. This implies a near perfect structure, close to the *maximum* preferred orientation which can be achieved by consolidation from an initially random structure. Hence the degree of orientation at the outset of the shear tests was virtually the most intense possible for the method of preparation of the clay. Nevertheless the shearing resistance of the clay remained independent of this original fabric. The original fabric is thought to correspond to the electron micrographs of a compressed flocculated kaolin given by West (1964). These reveal that although a strong preferred orientation is obtained significant local departures persist.

Shear strength

Consideration may now be given to the interpretation of the mechanics of the shear-box test itself. Neglecting edge effects and assuming constant volume deformation, three alternative interpretations are current (Hansen, 1961). The most common interpretation assumes that the shear strength is mobilized in the direction of the apparent shear stress. This direction is a slip line and its conjugate is inclined at $(90° - \phi)$ to the horizontal. If there is no cohesion, the ratio τ_a/σ_{n_a} gives tan ϕ directly and the principal stresses are inclined as shown in Fig. 21(a). Hill (1950) pointed out that the direction of the apparent shear stress is the direction of the maximum shear strain rate, and if the axes of principal stress coincide with those of strain rate then this shear stress is the maximum shear stress. The ratio τ_a/σ_{n_a} now gives sin ϕ directly. As elucidated by Hansen (1961) the conjugate slip lines are inclined at $\phi/2$ and $(90° - \phi/2)$ to the horizontal. This interpretation is illustrated in Fig. 21(b). It is the same as assuming simple shear conditions to exist. However, if the axes of principal stress deviate by $\phi/2$ from the axes of principal strain rate, the original interpretation is recovered in terms of stresses while the horizontal is still the direction of maximum shear strain rate. The possibility of such a deviation is the result of the kinematic model introduced by Josselin de Jong (1959). The interpretation of the shear box test for this third alternative is given in Fig. 21(c).

Gibson (1953) showed that the inclination of slip planes in cylindrical samples at peak stress is best predicted by the Mohr–Coulomb failure criterion in terms of the Hvorslev strength parameters and that the Hvorslev angle of shearing resistance (ϕ_e) of a kaolin is almost equal to its angle of shearing resistance in terms of effective stress. The kaolin used in these experiments is rather coarse grained and it would have almost zero true cohesion. Its ϕ_e may be assumed equal to the peak angle of shearing resistance (ϕ_p) which is 24°. Therefore if at peak stress in the kaolin specimens subject to direct shear slip planes are found at 12° and conjugates at 78° to the horizontal, the interpretation of the shear box advocated by Hill (1950) and Hansen (1961) would be supported and simple shear would exist at peak.

The strength at peak is obtained by adjusting the apparent shear stress to account for that portion of the horizontal mid-plane which at the edges contains a displacement discontinuity (e.g. Fig. 5). The residual strength is assumed to act along this length and the adjusted shear stress acts in the central portion of the specimen. The residual strength has been obtained by shearing a specimen with a pre-cut plane. The stress-displacement curve is shown in Fig. 4 and the residual angle of shearing resistance (ϕ_r) is 12·2°. This value is close to that obtained from reversal tests by Kenney (1966) for a coarser kaolin. The adjustment

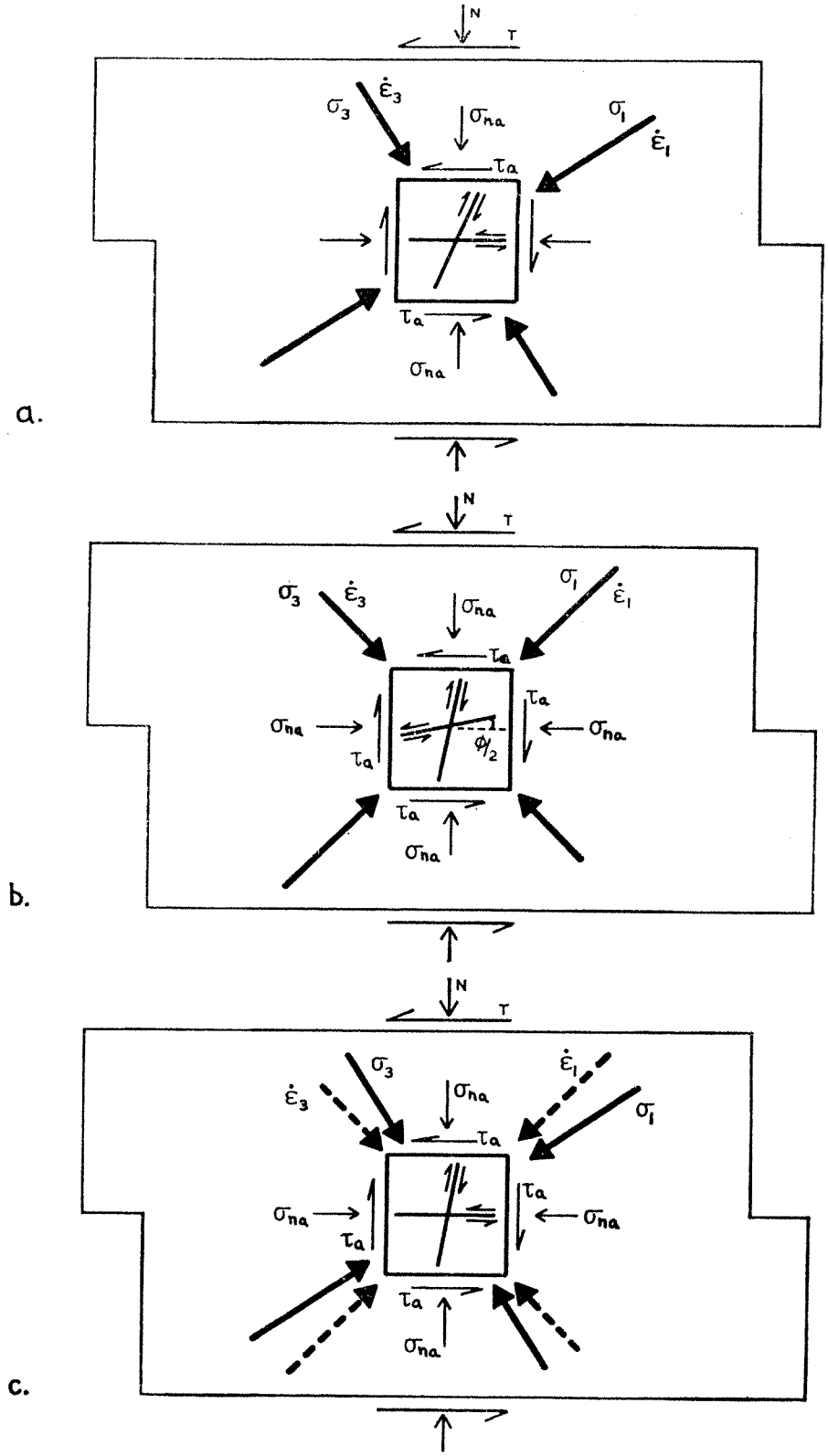

Fig. 21. Interpretation of the shear box test. Stress and strain rate directions in
(a) the common interpretation
(b) the Hill (1950) and Hansen (1961) interpretation
(c) the interpretation based on Josselin de Jong (1959)

Table 1. Interpretation of angles of shearing resistance

Position and method	Adjusted	Unadjusted
Peak, $\tau/\sigma_n = \sin\phi$ — — —	24°	21·4°
Peak, $\tau/\sigma_n = \tan\phi$ — — —	22·4°	20°
Pre-cut plane, $\tau/\sigma_n = \tan\phi_r$ — —	—	12·2°

increases the shear stress by 12%. The angle of shearing resistance of 24° has been computed from

$$\tau_a/\sigma_{n_a} = \sin\phi \quad . \quad . \quad . \quad . \quad . \quad . \quad . \quad . \quad . \quad (1)$$

Table 1 contains adjusted and unadjusted values calculated using equation (1) and the more conventional interpretation which is

$$\tau_a/\sigma_{n_a} = \tan\phi \quad . \quad . \quad . \quad . \quad . \quad . \quad . \quad . \quad . \quad (2)$$

The value of 24° is supported by measurements of the inclination of shear planes in both unconfined compression tests and Cloos–Riedel experiments (Tchalenko, 1967).

Peak structures

In both families of tests described the major structures formed at or near peak strength were inclined at 12° to the horizontal and at 80°–85° to the horizontal. Therefore the kinematic features are best interpreted in terms of simple shear with the high angle conjugate features having been somewhat rotated together with S_1. As Cloos (1955) has observed, discontinuities which are at a larger angle to the motion rotate more than the features nearly parallel to the motion. The stresses in the central portion of the specimen are as shown in Fig. 22(a).

Restraint structures

If there were no restraint against motion in the S_2 direction slip would continue as the strength dropped to the residual along this discontinuity and no new structures would be observed. Denoting the strength mobilized along this discontinuity by ϕ_m, where

$$\phi_p \geq \phi_m \geq \phi_r \quad . \quad . \quad . \quad . \quad . \quad . \quad . \quad . \quad . \quad (3)$$

the apparent resistance (ϕ_a) that would be observed in unrestrained simple shear is given by

$$\sin\phi_a = \frac{\tan\phi_m\,(1+\tan^2\phi_p/2)}{1-\tan^2(\phi_p/2)+2\tan(\phi_p/2)\tan\phi_m} \quad . \quad . \quad . \quad . \quad (4)$$

However, sustained motion along S_2 cannot occur although it is suggested that sufficient slip is possible to reduce the resistance in this direction towards the residual strength. Because of this kinematic restraint the principal stresses must change in magnitude and direction.

As mentioned in the observations on specimens sheared normal to S_1, the S_3 which forms directly after S_2 is bounded by strain discontinuities inclined at −15°. Any interpretation of the stresses after peak must be consistent, at least locally, with the attitude of S_3. Since the stress distribution is not known theoretically or experimentally, assumptions must be made to explain the observations. The simplest assumption, which is favoured here, is that subject to edge corrections, the stresses which are measured throughout the experiment are the normal and shear stresses acting on a horizontal plane. Now if discontinuities are to appear in a new direction, virgin material must be stressed to the peak resistance even though the specimen as a whole displays unstable yielding. If the normal and shear stress acting on a horizontal plane are known it is always possible to construct a Mohr's circle tangent to the failure envelope by a suitable choice of the horizontal normal stress. For the restraint stuctures considered

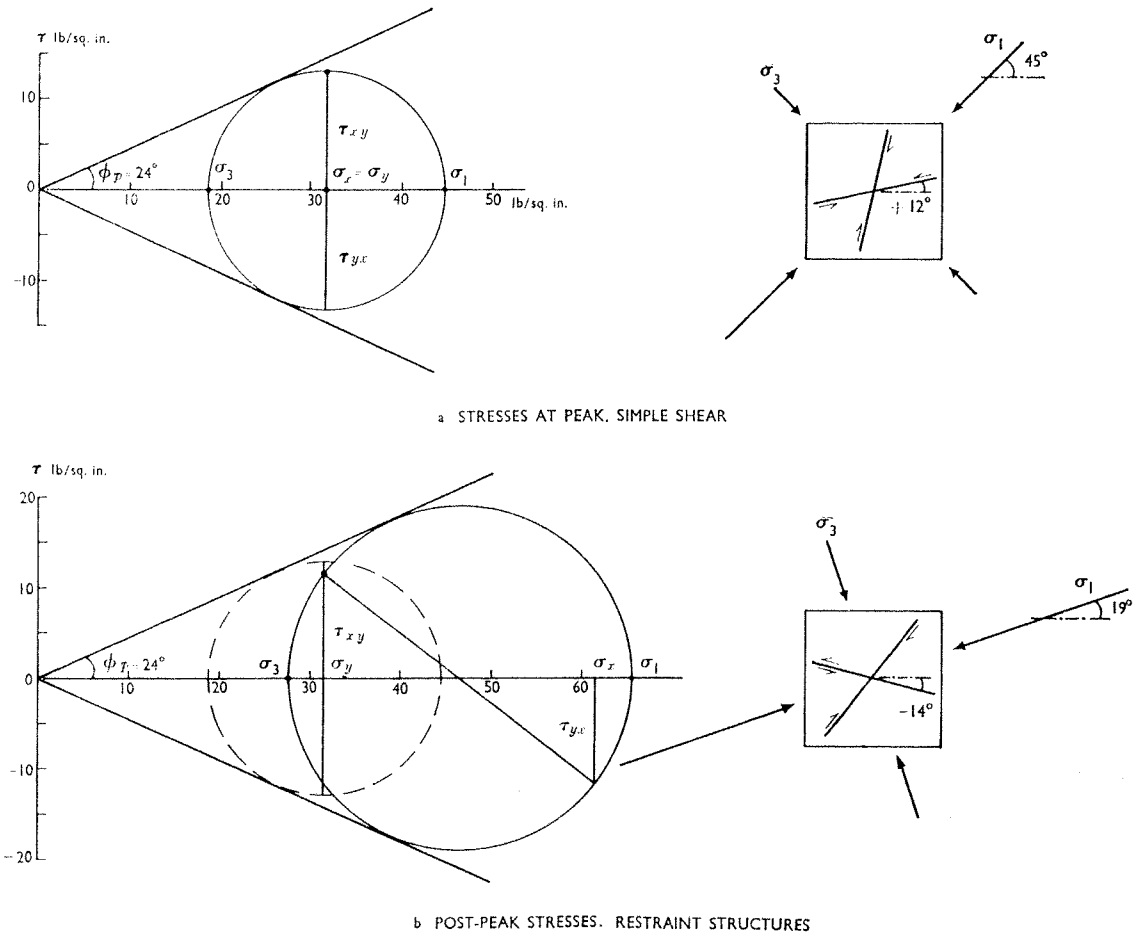

Fig. 22. Stresses and failure directions for a central element

here this involves an increase in this stress and therefore both an increase and rotation of the principal stresses.

Specimen V5 (see Fig. 4) was deformed to a point on the unstable portion of the stress–displacement curve. The adjusted shear stress at this point is 11·8 lb/sq. in. and the stresses compatible with this value and causing failure in a new direction are shown in Fig. 22(b). The major principal stress has increased considerably and rotated to 19° to the horizontal. The predicted inclination of the new discontinuity is −14° which is close to the inclination of the boundary of S_3.

Since all the stresses acting on an element are known at the instant of the formation of S_3, it is possible to compute the shear stress and normal stress acting on the S_2 plane. The resistance in the S_2 direction must exceed the stresses. If the material is stable, this would always be so. However, if a reduction occurs in the strength along S_2 before the development of the restraint, it is of interest to compare the strength required to deter motion along S_2 with the strength that may be available. The required resistance, denoted by ϕ_n, may be found from

$$\frac{\sigma_x}{\sigma_{n_a}} = \frac{\sin\phi_a + (\sin\phi_a \tan\phi_n + 1)\tan(\phi_p/2) - \tan^2(\phi_p/2)\sin\phi_a - \tan\phi_n + \sin\phi_a \tan\phi_n \tan(\phi_p/2)}{\tan(\phi_p/2) + \tan\phi_n \tan^2(\phi_p/2)} \tag{5}$$

The terms in equation (5) are defined in Fig. 23.

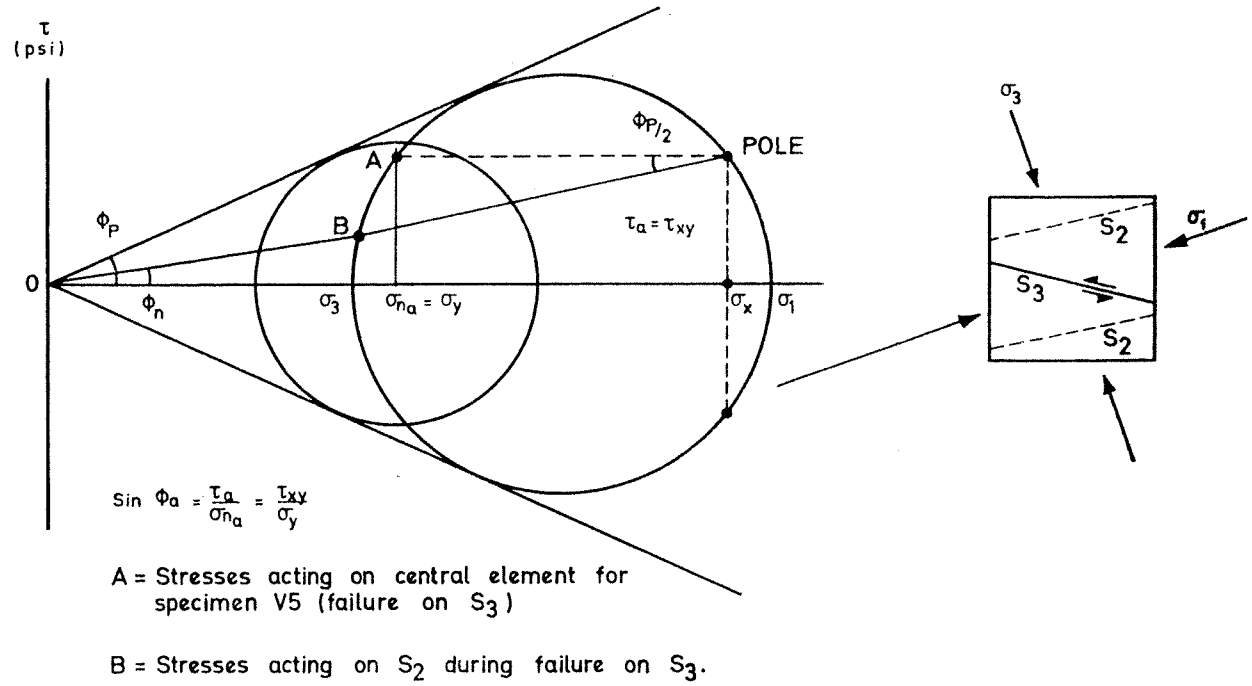

Fig. 23. Stresses acting on the peak structure during failure in the restraint direction

For specimen V5, ϕ_n is 10°. This is less than the lowest possible resistance in the S_2 direction which is 12·2° and therefore the restraint mechanism is at least consistent with the properties of the kaolin. However, an argument against this restraint hypothesis becomes evident. It is possible to imagine a specimen of some material in the shear box which has a resistance in the S_2 direction less than that computed from equation (5). This could arise either through a large difference between cohesions of intact and sheared material or through a large difference between the angles of shearing resistance. Although kinematic restraint would still persist, to account for the orientation of the new discontinuities it is necessary to know the stresses associated with the real boundary conditions.

For specimens with an initially horizontal S_1, the restraint structures are composed of S_{3c} inclined at −20° and its coalescence which forms S_4. The initial stages of the development of this structure are shown in Fig. 18.

Kink-bands and related structures

Many features of structures depend upon the orientation of S_1. Where S_1 is sub-horizontal, and hence favourably aligned for motion in the direction of shear, S_{3b} is thin with no discernible sub-structure except the intense orientation of the particles composing it. However, its conjugate, S_{3a}, separates much thicker domains within which sub-structures have been observed. When S_1 is sub-vertical, S_2 is thick and contains a well-defined sub-structure. Its conjugate is in this case only a thin discontinuity.

The rotation of S_1 between two parallel strain discontinuities results in a kink-band. From studies on the deformation of foliated rocks (e.g. Dewey, 1965) it is possible to distinguish between normal and reverse kink-bands. A normal kink-band occurs when the rotation of S_1 within it decreases the original acute angle of S_1 with respect to the direction of the strain discontinuities. When this angle increases, the structure is termed a reverse kink-band.

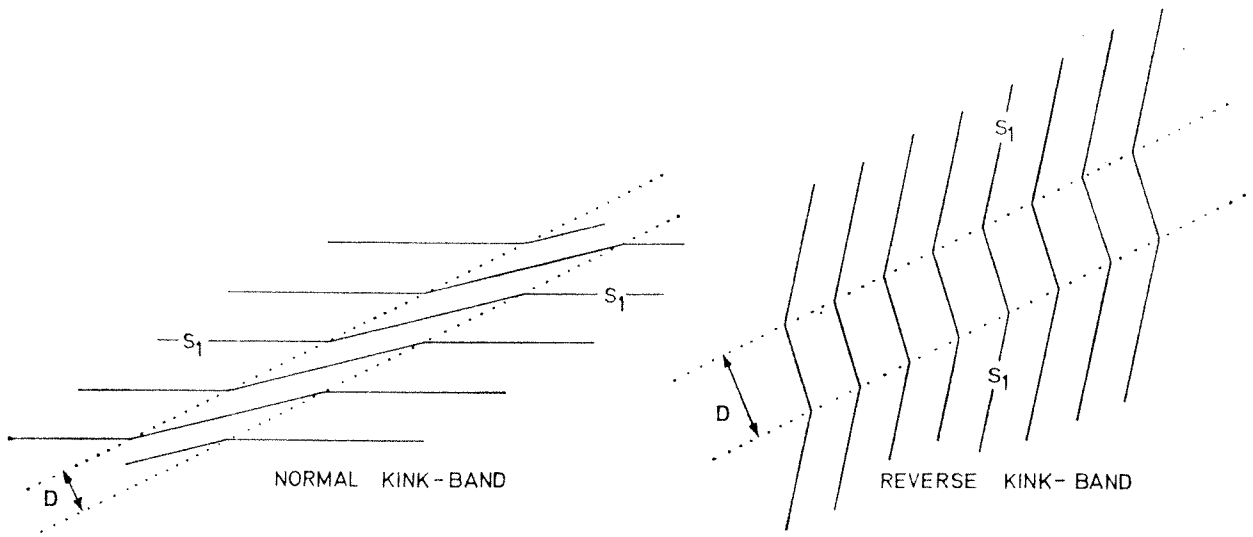

Fig. 24. Types of kink-band

This distinction is illustrated in Fig. 24. If the width D of the kink-band is fixed, the action of a normal kink-band is to produce initially a shortening normal to the preferred orientation while that of a reverse kink-band is to produce an elongation in this direction.

Both S_{3b} for the set of tests containing an initially horizontal S_1 and S_{2a} and S_{3a} for the other series are normal kink-bands. For these cases only a small local rotation of S_1 produces the structure. The normal kink-band S_{3b} is an active structure and after some slip has occurred, displacement discontinuities composed of particles parallel to it form the boundaries in the directions of the two strain discontinuities. The particle orientation between these two discontinuities is not parallel to the boundaries. However, optical measurements show that the degree of orientation has been enhanced.

For the series of tests with a horizontal S_1, the penetrative structure formed by S_{3a} (Fig. 17) is a family of reverse kink-bands. S_2 in the vertical set is also a reverse kink-band. The sequence of the initial stages of the development of S_2 is not wholly clear. There is some evidence that the discontinuities S_{2b} form as an *en echelon* family of small kink-bands before the overall rotation of S_1 within S_2. Such a family has been noted in shales of the East Transvaal by Ramsay (1962).[9] However, most of our observations are consistent with the double strain discontinuity S_2 preceding the development of S_{2b}. The rotation of S_1 within S_2 is arrested when the kink-band boundary bisects the angle formed by the S_1 directions on either side of it. If the thickness of the kink-band is kept fixed rotation beyond this point requires a compression normal to S_1 within the band. The S_{2b} structures form at approximately $\phi_p/2$ to S_2, and they subsequently coalesce to form the displacement discontinuity S_{2d}.

For the initial fabrics under consideration, when one structure, say S_2, is a normal kink-band its conjugate structure, S_{2a}, is a reverse kink-band. For the horizontal S_1 series, the conjugate shear direction is nearly normal to the basal planes of the particles and since basal plane slip cannot take place in this direction the conjugate shear stress induces the kink-band S_{3a}. The formation of such a structure is the result of mechanical instability and no detailed interpretation can be given for it. Paterson and Weiss (1966) have discussed these difficulties.

[9] A sketch is given in Fig. 8 of this reference. The interpretation of the mechanics given in this Paper is not under consideration here.

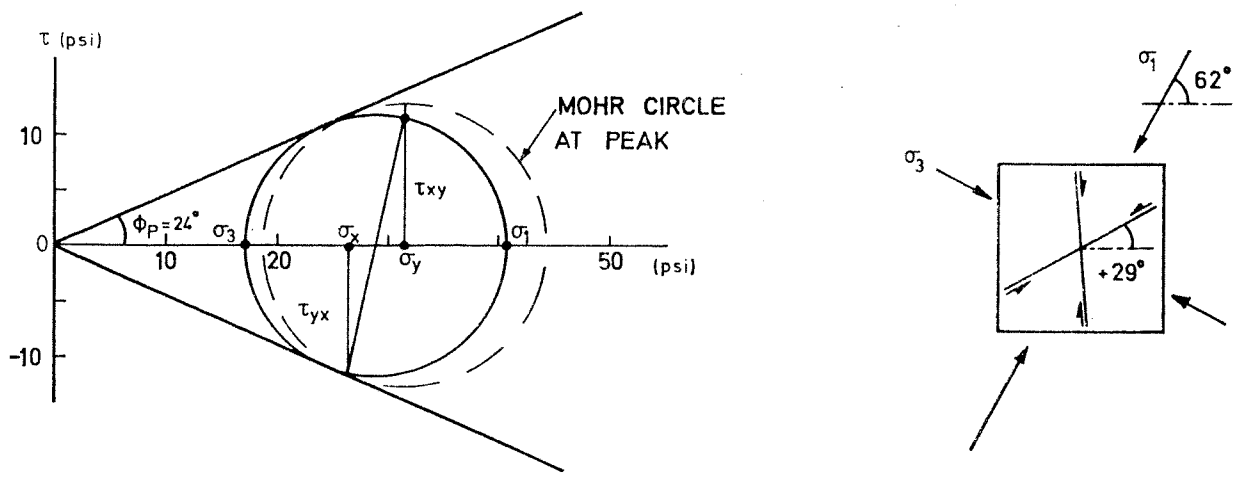

Fig. 25. Stresses and failure directions for a central element. Relief structure

Relief structures

Some of the structures which appear within a kink-band present a special problem. As mentioned previously, in the case where S_2 is a reverse kink-band (vertical S_1), S_{2b} is understood to form after the bounding strain discontinuities. The attitude of S_2 at $\phi_p/2$ to the horizontal is consistent with failure under simple shear conditions. Since S_{2b} is at ϕ_p to the horizontal a different mechanism must operate within S_2. It is suggested that this mechanism is like that causing the restraint structures but involves instead a decrease in horizontal normal stress. Taking the apparent shear strength to be slightly less than peak, it is possible to draw a stress circle tangent to the failure envelope with a horizontal normal stress less than that which would exist under simple shear. This is shown in Fig. 25 and predicts a new discontinuity at about ϕ_p to the horizontal. Only a small local decrease in the horizontal normal stress is necessary to achieve this state. The reason for this is not obvious. S_{3d} in the penetrative kink-band is also at $\phi_p/2$ to the boundaries of the kink-band and is therefore probably a relief structure.

Ultimate structure

At the end of travel of the shear box, the ultimate structure governing the residual strength has not been achieved. The last structure observed in either series of tests, S_4, consists of displacement discontinuities joining operative components of S_2 and S_3. The continuous slip surface so formed is distinctly wavy and it may be assumed that further displacement along it would reduce the irregularities. Generally the particle forming the displacement discontinuity are initially at an angle of 0 to $-15°$ to it. Where these displacement discontinuities evolve further they are composed of two thin bands of particles at their periphery aligned in the direction of motion, separating a thicker highly orientated band with particles aligned at -40 to $-50°$. This internal structure has been called a compression texture by Morgenstern and Tchalenko (1967c). The basal planes are approximately normal to the major principal stress.

This ultimate structure has also been produced by testing a specimen with an originally vertical S_1 containing a horizontal plane cut normal to the direction of shear. A detail of the shear zone is given in Fig. 26. The stress-displacement relation for this specimen has been given in Fig. 4. Although no detailed explanation for the compression texture can be given at present, similar features have been observed during friction and wear studies on a variety of materials (e.g. Alison, Stroud and Wilman, 1965).

CONCLUSIONS

The preparation of the kaolin used in these tests resulted in an original fabric prior to shearing which had as well-developed a degree of orientation as can be achieved by consolidation from an initially flocculated state. Nevertheless, the response of this material to direct shear displayed only a small anisotropy of strength. Since the true cohesion of kaolin is known to be very small this quasi-isotropic behaviour cannot be attributed to an isotropic distribution of cohesive bonds. Moreover, the specimen containing a cut plane had a considerably reduced shearing resistance which is consistent with the known influence of particle orientation on the strength of clays. It is therefore concluded that although the average particle orientation is very strong there are sufficient local deviations from it to deter the clay from failing at the residual strength from the outset. Virtually perfect particle alignment is necessary in a kinematically admissible direction to obtain the residual angle of shearing resistance.

Particular attention has been paid to the shear-induced fabric. All the components observed may be accounted for by some combination of basal-plane gliding producing translation and rotation. The development of displacement discontinuities across a particle does not appear to be a possible mode of motion, presumably because of the high relative strength of the particles. Imposed irreversible deformations must be accommodated by rigid-body movements of the clay particles.

Although the stress and displacement conditions in the shear box are non-homogeneous, many aspects of the shear-induced fabric under these conditions are reproducible and amenable to interpretation. During stable yielding to peak strength, no discontinuities appear. The only observed feature is a quasi-homogeneous rotation of S_1 in the direction of the imposed motion. The amount of rotation depends upon the initial orientation of S_1.

The structures which appear at or near the peak strength indicate that the central portion of the specimen is in simple shear. This confirms the interpretation of the shear box suggested by Hill (1950). The major structures which appear are Riedel shears whose attitude is governed by the Hvorslev angle of shearing resistance. Since these structures are oblique to the horizontal, kinematic restraint is an important feature of the shear box. A mechanism has been suggested to account for the subsequent structures which correctly predicts their inclinations.

A study of the sub-structures reveals that kinking is the dominant mode of deformation in the production of the major structures. Sub-structures within kink-bands also appear. Many features of the kink structures are comparable to full-scale geological structures. Although interpretations have been offered for some aspects of the sub-structures, other features are not understood. Examples for which no explanation has been given are the instability which produces a penetrative kink-band, and the development of particle orientation normal to the major principal stress in the ultimate structure.

It is clear that further structural studies are necessary. Such studies will not only elucidate the role of discontinuities in the deformation of soils but will also provide basic information that any continuum theory must consider. It may be anticipated that these studies will go a considerable distance to unify our understanding of the behaviour of soils with that of rocks on a megascopic scale and that of single and polycrystals on a microscopic scale.

ACKNOWLEDGEMENTS

The Authors are grateful for the support given to this study by the Natural Environment Research Council. They also wish to acknowledge the encouragement and advice offered by Professor A. W. Skempton and Dr N. N. Ambraseys. The assistance of Miss J. Gurr with the photography has been invaluable.

REFERENCES

ALISON, P. J., STROUD, M. F. & WILMAN, H. (1965). Abrasion of metals and binary alloys. *Proc. Third Conf. Lubrication and Wear*, pp. 50–61. Instn. mech. Engrs.

ASTBURY, N. F. (1960). Science in the ceramic industry. *Proc. R. Soc.*, A **258**, 27–46.

BISHOP, A. W. (1966). The strength of soils as engineering materials. *Géotechnique* **16**, 91–128.

BISHOP, A. W., WEBB, D. L. & LEWIN, P. I. (1965). Undisturbed samples of London Clay from the Ashford Common shaft: strength-effective stress relationships. *Géotechnique* **15**, 1–31.

CHENEVERT, M. E. & GATLIN, C. (1965). Mechanical anisotropies of laminated sedimentary rocks. *J. Soc. Petrol. Engrs* **5**, 67–77.

CLOOS, E. (1955). Experimental analysis of fracture patterns. *Bull. geol. Soc. Am.* **66**, 241–256.

DEWEY, J. F. (1965). Nature and origin of kink-bands. *Tectonophysics* **1**, 459–494.

DUNCAN, J. M. & SEED, H. B. (1966a). Anisotropy and stress re-orientation in clay. *Proc. Am. Soc. civ. Engrs* **92**, SM5, 21–50.

DUNCAN, J. M. & SEED, H. B. (1966b). Strength variation along failure surfaces in clay. *Proc. Am. Soc. civ. Engrs* **92**, SM6, 81–104.

GIBSON, R. E. (1951). An investigation of the fundamental shear strength characteristics of clay. Ph.D. Thesis, University of London.

GIBSON, R. E. (1953). Experimental determination of the true cohesion and true angle of internal friction in clays. *Proc. Third Int. Conf. Soil Mech.* **1**, 126–130.

GOLDSTEIN, M. N., MISUMSKY, V. A. & LAPIDUS, L. S. (1961). The theory of probability and statistics in relation to the rheology of soils. *Proc. Fifth Int. Conf. Soil Mech.* **1**, 123–126.

HANSEN, B. (1961). Shear box tests on sand. *Proc. Fifth Int. Conf. Soil Mech.* **1**, 127–131.

HILL, R. (1950). *The mathematical theory of plasticity*. Oxford: Clarendon Press.

HVORSLEV, M. J. (1960). Physical components of the shear strength of saturated clays. *Proc. Res. Conf. Shear Strength Cohesive Soils*, 437–501. Am. Soc. civ. Engrs.

JOSSELIN DE JONG, G. (1959). *Statics and kinematics in the failable zone of a granular material*. Delft.

KENNEY, T. C. (1966). Residual strength of fine-grained minerals and mineral mixtures. *N.G.I.*, Pub. No. 68, 53–58.

KISIEL, J. (1964). On experience acquired in the course of tests carried out with a shear box. *Archwm Hydrotech.* **11**, 415–421.

LAFEBER, D. & KURBANOVIC, M. (1965). Photographic reproduction of soil fabric patterns. *Nature* **208**, 609–610.

MITCHELL, J. K. (1956). The fabric of natural clays and its relation to engineering properties. *Proc. Highw. Res. Bd* **35**, 693–713.

MORGENSTERN, N. R. & TCHALENKO, J. S. (1967a). The optical determination of preferred orientation in clays and its application to the study of microstructure in consolidated kaolin, I. *Proc. R. Soc.*, A **300**, 218–234.

MORGENSTERN, N. R. & TCHALENKO, J. S. (1967b). The optical determination of preferred orientation in clays and its application to the study of microstructure in consolidated kaolin, II. *Proc. R. Soc.*, A **300**, 235–250.

MORGENSTERN, N. R. & TCHALENKO, J. S. (1967c). Microstructural observations on shear zones from slips in natural clays. *Proc. Geotechnical Conf.*, pp. 147–152. Oslo.

O'BRIEN, N. R. (1963). A study of fissility in argillaceous rocks. Ph.D. Thesis, University of Illinois.

PATERSON, M. S. & WEISS, L. E. (1961). Symmetry concepts in the structural analysis of deformed rocks. *Bull. geol. Soc. Am.* **72**, 874.

PATERSON, M. S. & WEISS, L. E. (1966). Experimental deformation and folding in phyllite. *Bull. geol. Soc. Am.* **77**, 343–374.

PETLEY, D. (1966). The shear strength of soils at large strains. Ph.D. Thesis, University of London.

RAMSAY, J. G. (1962). The geometry of conjugate fold systems. *Geol. Mag.* **99**, 516–526.

ROSENQUIST, I. Th. (1959). Physical-chemical properties of soils. *Proc. Am. Soc. civ. Engrs* **85**, SM2, 31–53.

SANDER, B. (1948). Einführung in die Gefügekunde des Geologischen Körper, I. Vienna: Springer.

SKEMPTON, A. W. (1964). Long-term stability of clay slopes. *Géotechnique* **14**, 77–101.

SKEMPTON, A. W. (1966). Some observations on tectonic shear zones. *Proc. First int. Congr. rock Mech.* **1**, 329–335.

TCHALENKO, J. S. (1967). The influence of shear and consolidation on the microscopic structure of some clays. Ph.D. Thesis, University of London.

TURNER, F. J. & WEISS, L. E. (1963). *Structural analysis of metamorphic tectonites*. New York: McGraw-Hill Co.

TUROVSKAYA, A. YA. (1964). The soil structure in shear zones. *Voproci Geotechniki* **7**, 57–68.

WEST, R. (1964). The characteristics of filter pressed kaolinite-water pastes. *Proc. Twelfth natn. Conf. Clays and clay Miner.*, pp. 209–222. New York: Pergamon.

WEYMOUTH, J. H. & WILLIAMSON, W. O. (1953). The effects of extrusion and some other processes on the microstructure of clay. *Am. J. Science* **251**, 89–108.

WILLIAMSON, W. O. (1947). The fabric, water-distribution, drying-shrinkage and porosity of some shaped discs of clay. *Am J. Sci.* **245**, 645–662.

YONG, R. N. & WARKENTIN, B. P. (1966). *Introduction to soil behaviour*. New York: Macmillan Co.